

# Formation of OTS self-assembled monolayers at chemically treated titanium surfaces

Elnaz Ajami · Kondo-Francois Aguey-Zinsou

Received: 21 July 2010 / Accepted: 23 May 2011 / Published online: 7 June 2011  
© Springer Science+Business Media, LLC 2011

**Abstract** Enhanced biocompatibility of titanium implants highly depends on the possibility of achieving high degrees of surface functionalization for a low immune response and/or enhanced mineralization of bioactive minerals, such as hydroxyapatite. In this respect, surface modification with Self Assembled Monolayers (SAMs) has a great potential in delivering artificial surfaces of improved biocompatibility. Herein, the effectiveness of common chemical pre-treatments, i.e. hydrogen peroxide ( $H_2O_2$ ) and *Piranha* ( $H_2SO_4 + H_2O_2$ ), in facilitating surface decontamination and hydroxylation of titanium surfaces to promote further surface functionalization by SAMs is investigated. The quality of the octadecyltrichlorosilane (OTS) based SAM appeared to strongly depend upon the surface morphology, the density and nature of surface hydroxyl sites resulting from the oxidative pre-treatments. Contrary to common belief, no further hydroxylation of the titanium substrate was observed after the selected chemical pre-treatments, but the number of hydroxyl groups available on the surface was decreased as a result of the formation of a titanium oxide layer with a gel-type structure. Further examinations by atomic force microscopy, infrared spectroscopy and X-ray photoelectron spectroscopy also revealed that mild oxidizing conditions were sufficient to remove surface contamination without detrimental effects on surface hydroxylation state and surface roughness.

Furthermore, the adsorption of the alkylsiloxane molecules forming the SAM film is believed to proceed through hydrolysis at surface acidic hydroxyl groups rather than randomly. This site dependent adsorption process has significant implications for further functionalization of titanium based implants. It also highlights the difficulty of achieving an OTS based SAM at the surface of titanium and question the quality of SAMs reported at titanium surfaces so far.

## 1 Introduction

Titanium and its alloys are widely used in orthopedic surgery as load bearing implants because of their superior mechanical properties, good biocompatibility with hard human tissues, and high resistance to corrosion [1]. Good osteointegration of a titanium implant will depend upon several factors including bio-recognition, bone growth and adhesion of the new bone at the implant surface. The later has appeared to be challenging due to slow rate of bone ingrowth in the early stages of post-implantation [2].

Different surface modifications based on mechanical, chemical and physical means have been pursued to facilitate bone growth onto the surface of titanium [3]. However, methods based on the modification of titanium surface with calcium phosphate and/or hydroxyapatite (HA) coatings have attracted most research interest because of the substantial improvements achieved in terms of osteointegration [4]. Among the different methods available to deposit HA onto titanium substrates, plasma-spray is the most widely used technique because of the relative simplicity of the process in producing commercial HA modified implants. Although the benefit of such HA coated implants is widely recognized, several poor characteristics of

---

E. Ajami · K.-F. Aguey-Zinsou  
School of Engineering and Materials Science, Queen Mary,  
University of London, London E1 4NS, UK  
e-mail: e.ajami@qmul.ac.uk

K.-F. Aguey-Zinsou (✉)  
School of Chemical Engineering, The University of New South  
Wales, Sydney, NSW 2052, Australia  
e-mail: f.aguey@unsw.edu.au

plasma-sprayed HA coatings include inconsistency in the structure of coating, phase and chemical composition, problems associated with bioresorption, degradation and bone apposition [5].

Ideally, the HA coating should satisfy specific requirements, including a high degree of crystallinity for appropriate biological response, consistent characteristics across the coating layer, good coating adhesion and optimal porosity to promote bone ingrowth. A surface induced mineralization method whereby HA mineralization is induced at molecular levels by a functional Self-Assembled Monolayer (SAM) is therefore a more promising approach [6]. SAMs carrying specific groups, such as carboxylic acid and phosphate, have been found to induce calcium phosphate and HA mineralization with high crystallinity and relatively strong interfacial bonds with the substrates [2, 7–10]. However most investigations were conducted on substrates such as silicon [10–13] and gold [14, 15], on which the formation of SAMs is relatively well understood. Further work has been reported on the mineralization of HA at SAMs modified titanium substrates [2, 6–9, 16, 17], but little attention has been paid to fundamental issues related to the formation of SAM based on silane chemistry. The functionalization of titanium surfaces with SAMs is usually carried out following basic procedures used for silicon, i.e. the surface of titanium is degreased with acetone, ethanol or toluene and further hydrocarbon contamination is removed using a *Piranha* solution (*v:v* H<sub>2</sub>SO<sub>4</sub>:H<sub>2</sub>O<sub>2</sub>). The later also supposedly contributes to further hydroxylation of the titanium substrate [18]. Evidently, the stability of the HA coating will depend on the strength and the organization of the SAM film at the surface of titanium. To obtain a well-ordered and densely packed SAM, the surface of the substrate should be relatively smooth, free from contaminants [19] and contain sufficient hydroxyl adsorption sites to achieve full coverage [7, 20]. A better understanding of the SAMs chemistry at titanium surfaces is therefore of importance.

Accordingly, this study aims at the rationalization of the influence of conventional chemical pre-treatments, including *Piranha* [21] and H<sub>2</sub>O<sub>2</sub> [22–24], and common experimental practices on the growth of SAMs at the surface of titanium. To this end, the commonly utilized and extensively investigated octadecyltrichlorosilane (SiCl<sub>3</sub>–(CH<sub>2</sub>)<sub>17</sub>–CH<sub>3</sub>) molecule has been used for the formation of SAMs. OTS bears only one reactive group to enable surface adsorption, i.e. SiCl<sub>3</sub>. Furthermore, the neutral terminal group (–CH<sub>3</sub>) of OTS reduces possible deformations of the SAM film due to steric repulsions of the end groups. Techniques, including scanning electron and atomic force microscopy, were used to characterize the morphological evolution of the surface of the substrate with respect to chemical pre-treatments and SAM growth. Further insight

into the evolution of the titanium surface chemistry upon chemical pre-treatments was gained by X-ray photoelectron spectroscopy, contact angle measurements and infrared spectroscopy.

## 2 Materials and methods

### 2.1 Materials

All chemicals, including acetone, ethanol (GPR grade), sulphuric acid (>97.5%, AR grade), hydrogen peroxide 30 wt. % in water (ACS reagent), OctadecylTrichloroSilane (OTS) (>90%), carbon tetrachloride (>99.8%) and chloroform (AR grade), were purchased from Sigma and used as received. IsoparG (mixture of branched iso alkanes C<sub>9</sub>–C<sub>12</sub> naphthenes, iso- and *n*-paraffins and alkanes) was bought from Exxon Chemical PF. Diamond suspensions, grinding papers and polishing mats were purchased from Buehler. Pure titanium plates (Ti) were purchased from Goodfellow and were cut to 1 × 1 cm<sup>2</sup> as the substrates.

### 2.2 Substrate pre-treatment

The substrates were first polished with a #800, #2400 and then a #4000 silicon carbide grinding paper using a Struers Knuth-Rotor grinding machine. Afterwards, the substrates were successively polished with 3, 1 and 0.25 μm polycrystalline diamond suspensions on velvet mats at 500 rpm. The polished substrates were sonicated in distilled water, ethanol and then acetone. They were finally blow dried with Ar. The polished substrates (Po-Ti) were treated using three different conditions: (a) immersed in a 2:1 *Piranha* solution (*v:v*, H<sub>2</sub>SO<sub>4</sub>: H<sub>2</sub>O<sub>2</sub>) at 60°C for 10 min (substrate denoted c\_Pi-Ti); (b) soaked at room temperature for 2 h in a *Piranha* solution diluted twenty times (substrate denoted as d\_Pi-Ti); or (c) dipped for 2 h at room temperature in a diluted solution of H<sub>2</sub>O<sub>2</sub>, i.e. 15 wt. % H<sub>2</sub>O<sub>2</sub> (substrate denoted as d\_HP-Ti). All the substrates were rinsed with a copious amount of distilled water and then blow dried with Ar.

### 2.3 SAM growth

The formation of the OTS self-assembled monolayer was carried-out following the procedure from Wang et al. [25], which does not require any specific facilities, such as a clean room. Nonetheless, SAM adsorption was carried out in a glove box under Ar atmosphere to avoid water polymerization of OTS. All experimental vessels and tweezers were thoroughly cleaned before use. A solvent mixture of 1 mL carbon tetrachloride, 1.5 mL chloroform and 10 mL IsoparG was dried over aluminum oxide (Fluka). A

micropipette was used to add OTS into the solvent to make a final OTS concentration of 10 mM. The Ti substrates were placed in 10 mL of OTS solution. The vials were tightly sealed and kept at 23°C for 24 h. The substrates were then removed from the OTS solution and successively sonicated in chloroform and ethanol for 5 min to remove any unbound OTS. They were finally blow dried with Ar and stored under Ar before characterization. Five substrates were prepared for each set of experimental conditions and the most representative results are reported.

#### 2.4 Scanning electron microscopy (SEM)

The surface morphology was characterized by Scanning Electron Microscopy (using a JEOL 6300 instrument) operated at 20 kV. The substrates were mounted and scanning electron micrographs were recorded at various magnifications.

#### 2.5 Atomic force microscopy (AFM)

Surface features were examined by atomic force microscopy. Measurements were performed in contact mode with a multimode scanning probe microscope from Veeco. The contact mode was chosen to avoid any artifact due to the water physisorbed at the surface of the Ti substrates. A silicon nitride cantilever with a spring constant of 0.05 N/m and resonance frequency of 22 kHz was used. The images were recorded with a resolution of  $300 \times 300$  pixels at a scanning rate of 1 Hz.

#### 2.6 X-ray photoelectron spectroscopy (XPS)

Evolution of the chemical composition of the titanium surface after chemical pre-treatment was determined by X-ray Photoelectron Spectroscopy (XPS) using a VG-Microtech Mutilab 3000 instrument. The specimens were mounted on standard sample stubs using double-sided adhesive tape. The XPS measurements were performed in a vacuum of less than  $10^{-7}$  Pa. An Al K $\alpha$  source with a power of 150 W was used. XPS spectral full scans and narrow scans for C1s, Ti2p and O1s were recorded.

#### 2.7 Contact angle measurements

The surface wettability of the titanium substrates was evaluated by contact angle measurements before and after chemical pre-treatment and modification by SAM. Experiments were carried out using high purity water and with a homemade instrument equipped with a Qx3 microscope from IntelPlay (Intel and Mattel) and a Kaiser RT1 camera. Five measurements were made at different locations on each substrate and the results were averaged.

#### 2.8 Diffuse reflectance infrared Fourier transform (DRIFT)

The formation of OTS based SAM at the surface of titanium and the level of order of the monolayer was evaluated by infrared spectroscopy using a DRIFT accessory. IR spectra were recorded using a Digilab instrument. The substrates were mounted on the stand within the DRIFT chamber. The signal was maximized and the spectra were recorded with 60 scans at a resolution of  $4 \text{ cm}^{-1}$ .

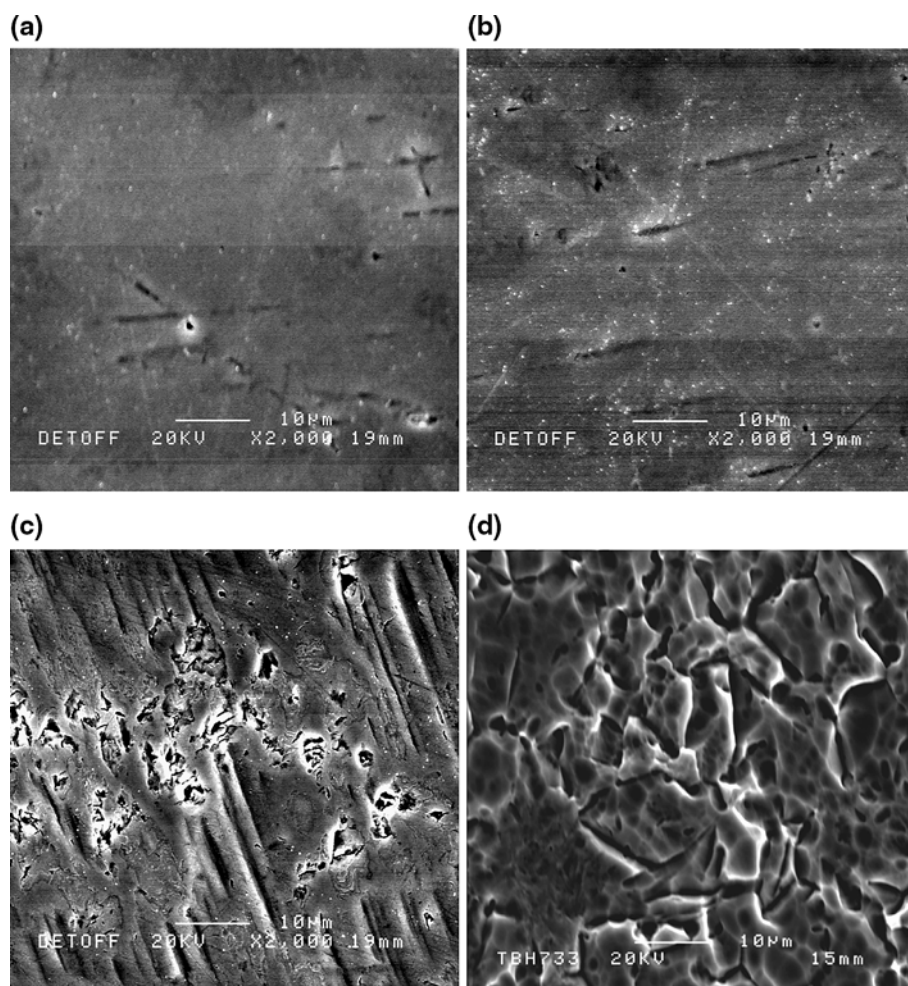
### 3 Results

#### 3.1 Effect of chemical pre-treatments on the surface properties of titanium

The titanium substrates initially polished (Po-Ti) were pre-treated with acidic solutions of different acidic strength and composition in order to remove organic contaminations and enhance surface hydroxylation prior to SAM functionalization. As shown in Fig. 1b, pre-treatment in *Piranha* solution resulted in severe surface etching and the formation of large crevices in comparison to the reference substrate (Po-Ti) (Fig. 1a). To mitigate the effect of *Piranha*, Po-Ti was treated with a 2:1 *Piranha* solution diluted twenty times and after such a treatment the surface remained relatively smooth (Fig. 1c). Similarly, pre-treatment of Po-Ti without sulphuric acid and with hydrogen peroxide only, to enhance surface hydroxylation, also resulted in the formation of a smooth surface with few crevices (Fig. 1d). Further characterizations by AFM confirmed the roughness observed by SEM at local levels. The Root Mean Square (RMS) roughness of Po-Ti was found to be only 1.5 nm (Fig. 2a). As observed by SEM and reported previously [18, 26, 27], the roughness of pre-treated Po-Ti with *Piranha* solution is relatively high, i.e. 30.6 nm (Fig. 2a, b). In comparison, pre-treatments with diluted *Piranha* solution (d\_Pi-Ti) and diluted hydrogen peroxide solution (d\_HP-Ti) led to an RMS of 2 and 6.6 nm, respectively (Fig. 2c, d). It is noteworthy that the horizontal noise observed as the AFM tip is dragged along the surface of d\_HP-Ti (Fig. 2d), would indicate a “soft” surface structure as further discussed below.

The evolution of surface chemistry of the substrates as a function of the pre-treatment method was characterized by XPS. The XPS survey spectra of the reference substrate, i.e. Po-Ti, and those after different treatments show peaks related to titanium, oxygen, and carbon (Fig. 3). The Auger peaks for Ti, O and C were also observed at higher binding energies. No sulphur peaks were detected by XPS analysis. Surface contamination by carbon was also determined by XPS. As shown in Fig. 4a, two main peaks were observed

**Fig. 1** SEM images of (a) Po-Ti, (b) d\_Pi-Ti, (c) d\_HP-Ti, and (d) c\_Pi-Ti. The scratches noticeable at the surface of Po-Ti are due to polishing effects



at 284.4 and 288.1 eV. These peaks correspond to C bonded with O (C–O, C=O and OH–C=O) [28–32], and hydrocarbons (C=C, C–C and C–H), [27, 33–35] respectively. Both peaks are due to CO<sub>2</sub> and organic contaminants, and their intensity was found to decrease with increased concentrations of the *Piranha* and in particular H<sub>2</sub>O<sub>2</sub>. Accordingly, the removal of carbon contamination from the titanium surface is mostly due to the use of H<sub>2</sub>O<sub>2</sub>, a strong oxidant, and not H<sub>2</sub>SO<sub>4</sub>.

These conclusions were confirmed by contact angle measurements (Fig. 5). The water contact angle of the pre-treated substrates was found to decrease from 75 down to 20° in agreement with previous studies [2, 7]. Furthermore, the following order of increasing hydrophilicity was observed: Po-Ti < d\_Pi-Ti < d\_HP-Ti ~ c\_Pi-Ti. This corresponds to the same trend observed for the evolution of carbon contamination as function of H<sub>2</sub>O<sub>2</sub> concentration (Fig. 4b). The lower the carbon contamination the higher is the surface hydrophilicity, suggesting once again that the increase in hydrophilicity is due to the decontamination of

the titanium surface and not further hydroxylation of the titanium surface, as believed previously [36].

The XPS narrow-scan spectra of Ti2p also revealed two main peaks at 458.8 and 464.4 eV, corresponding to TiO<sub>2</sub> (Fig. 6) [34, 35, 37, 38]. The weaker peak found at a lower binding energy of 453.0 eV was assigned to Ti<sup>0</sup> [39]. Since the intensity of this peak decreases in the following order: d\_Pi-Ti > d\_HP-Ti > c\_Pi-Ti, it can be concluded that at equivalent penetration depth of the photoelectrons (i.e. 7 nm), the thickness of the oxide layer is larger at c\_Pi-Ti than d\_Pi-Ti. Hence, the etching kinetic of the oxide layer should be slower in solutions of weaker acidic strength. Furthermore, the XPS narrow-scan spectra in O1s region revealed several peaks at 529, 530 and 531 eV, which were attributed to oxygen in bulk TiO<sub>2</sub> (Ti–O) [31, 32, 40], surface acidic and basic hydroxyl (OH) groups, respectively (Fig. 7) [37, 40, 41]. The acidic OH (OH<sub>a</sub>) is bound to two surface titanium atoms, whereas the basic OH (OH<sub>b</sub>) is bound to one surface titanium atom [42]. The XPS results in the O1s region are summarized in Table 1. In all

**Fig. 2** AFM images ( $5\ \mu\text{m} \times 5\ \mu\text{m}$ ) of (a) Po-Ti, (b) d\_Pi-Ti, (c) d\_HP-Ti, and (d) c\_Pi-Ti. Area RMS roughness: 1.5 nm for (a), 2.0 nm for (b), 6.6 nm for (c), and 30.7 nm for (d)

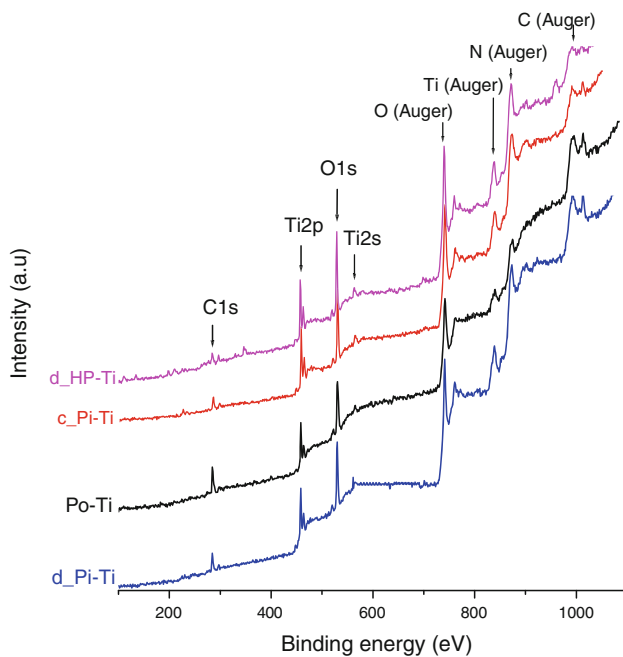
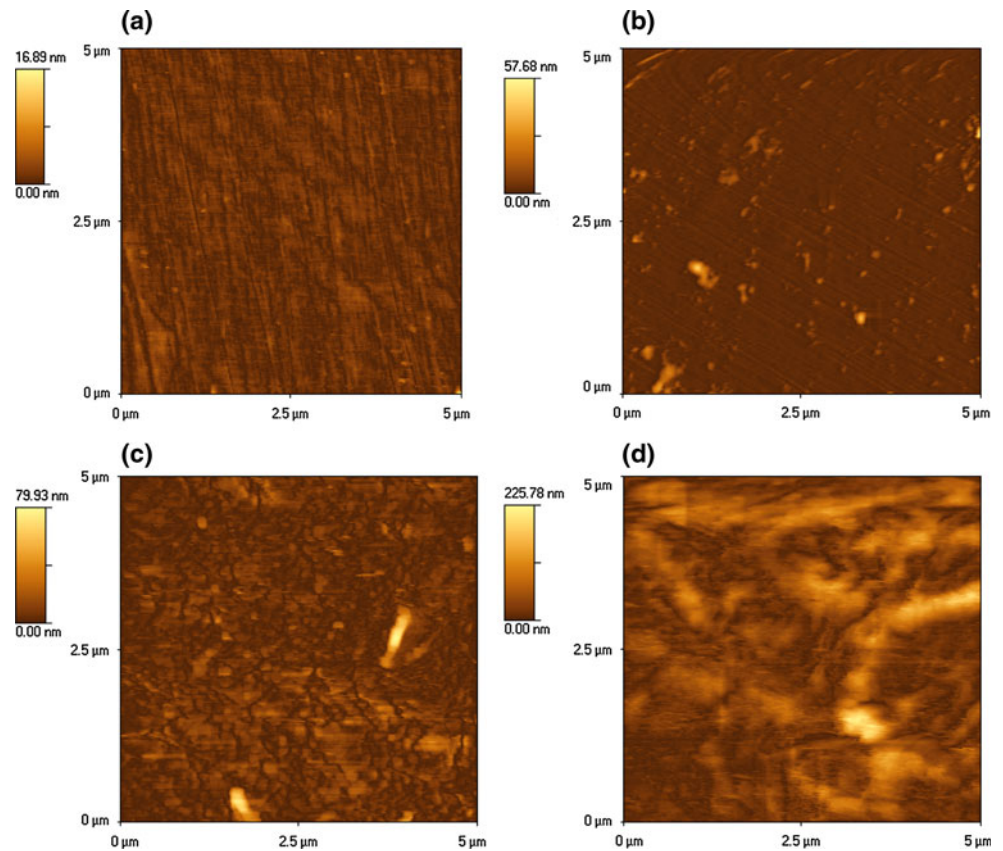


**Fig. 3** XPS wide-scan spectra of the untreated (Po-Ti) and treated titanium substrates (d\_Pi-Ti, d\_HP-Ti, and c\_Pi-Ti)

cases, the major contribution to the O1s peak resulted from Ti–O and it is noteworthy that the amount of OH groups was found to decrease in favor of the formation of Ti–O.

This result conflicts previous statement assuming that chemical oxidation facilitates the hydroxylation of titanium [7]. The reason for such a conflict may be due to the technique used, as a decrease in water contact angle at a titanium surface treated with *Piranha* [7] is not sufficient to guarantee the formation of surface hydroxyls. The removal of organic contaminants would also result in a decrease in surface tension. Furthermore, the contribution of OH<sub>a</sub> to the O1s peak appeared to be higher than that of OH<sub>b</sub>. Comparison of d\_Pi-Ti and c\_Pi-Ti shows that almost no OH<sub>b</sub> remained after treatment of the titanium substrate with a concentrated *Piranha* solution; however the amount of OH<sub>a</sub> increased. Consequently, treating titanium with the *Piranha* solution favored the formation of OH<sub>a</sub> in detriment to OH<sub>b</sub>. For the titanium substrate treated with diluted H<sub>2</sub>O<sub>2</sub>, such an effect was not observed and the amount of OH<sub>b</sub> is almost half that of OH<sub>a</sub>. This is in agreement with data reported by Matsumura et al. [43] showing that the amount of OH<sub>b</sub> decreases considerably after treatment of titanium with H<sub>2</sub>O<sub>2</sub>. During the competing dissolution of the oxide layer and further precipitation of titanium oxide, the surface is likely to undergo major reconstruction leading to the formation of an amorphous titanium oxide layer with a gel-like structure [22–24]. The decreased number of OH groups observed by XPS could result from a lower number of oxygen defective sites within the titanium

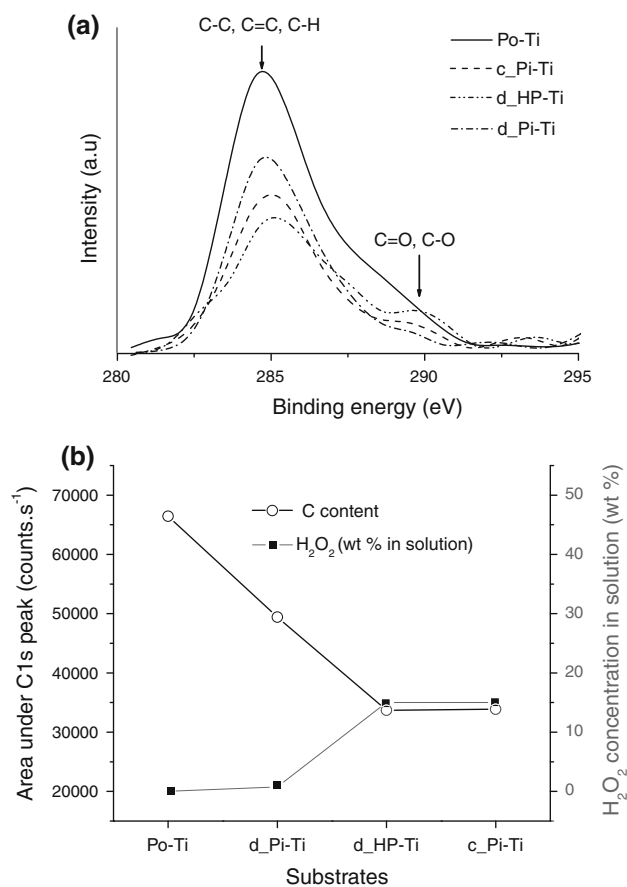


**Fig. 4** (a) XPS narrow-scan spectra of C1s and (b) level of carbon contamination on the titanium substrates as function of the pre-treatments used and associated H<sub>2</sub>O<sub>2</sub> concentration

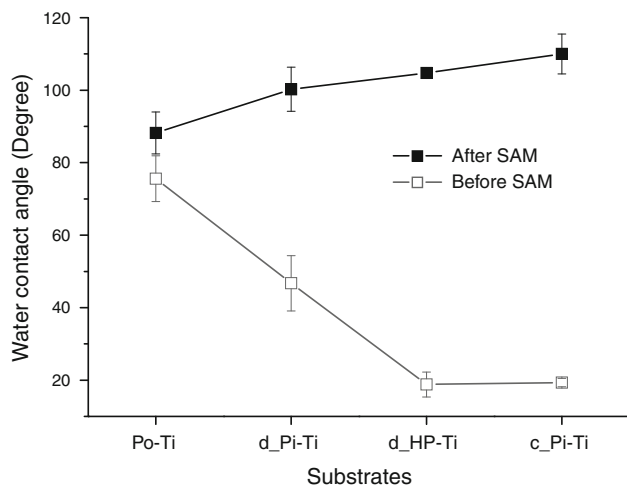


**Fig. 5** Water contact angle of chemically pre-treated titanium substrates before and after OTS adsorption

oxide gel layer, which in turn lowers the probability of forming OH<sub>a</sub> and OH<sub>b</sub> groups through dissociative water adsorption [44–46]. In addition, OH<sub>a</sub> and OH<sub>b</sub> on anatase powder were found to have a pK<sub>a</sub> of 2.9 and 12.7,

respectively [31, 42]. Assuming similar pK<sub>a</sub> values at the surface of titanium substrates, in a highly concentrated acidic medium, OH<sub>b</sub> is prone to dissociation leaving the surface with OH<sub>a</sub> groups only.

### 3.2 Formation of an OTS monolayer at titanium surfaces

The formation of SAM on the surface of titanium substrates was characterized by water contact angle measurements. As shown in Fig. 5, the hydrophilicity of the substrates substantially decreased from 20° to values in between 100 and 110° after immersion of the titanium substrates in the OTS solution. A similar value of 110° of water contact angle has been previously reported for the formation OTS monolayers fully covering the surface of silicon [25, 47, 48]. However, this result does not necessarily mean that a dense and well organized film has been formed. An increase in hydrophobicity would either be observed when the OTS molecules are well-organized into a dense and vertically oriented film or adsorbed at the surface of titanium in a disorganized structure with OTS molecules lying down on the surface. Furthermore, excessive roughness of the oxide layer, i.e. above 2.6 nm corresponding to the length of a fully stretched OTS molecule, would also lead to the accumulation of OTS molecules within the porosity of the surface and a certain level of conformational disorder within the OTS film.

In order to gain further insight in the structure of the OTS film, AFM investigations were carried out on the substrates with relatively smooth surfaces, i.e. Po-Ti and d\_Pi-Ti before and after OTS adsorption (Fig. 8). It was not possible to characterize the morphology of c\_Pi-Ti and d\_HP-Ti by AFM because of their relatively high surface roughness. Upon AFM imaging, the surface of Po-Ti

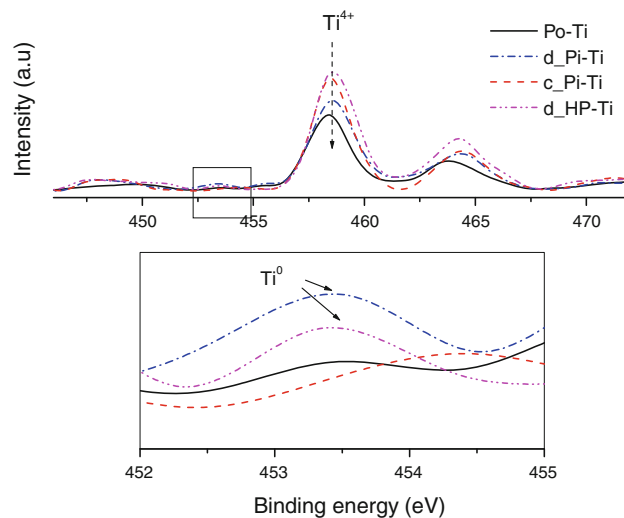


**Fig. 6** XPS Narrow-scan spectra of Ti2p of the titanium substrates

**Fig. 7** XPS narrow-scan of O1s for (a) Po-Ti, (b) d\_Pi-Ti, (c) d\_HP-Ti, and (d) c\_Pi-Ti. OH<sub>a</sub> stands for the surface acidic hydroxyl groups and OH<sub>b</sub> stands for the surface basic hydroxyl groups

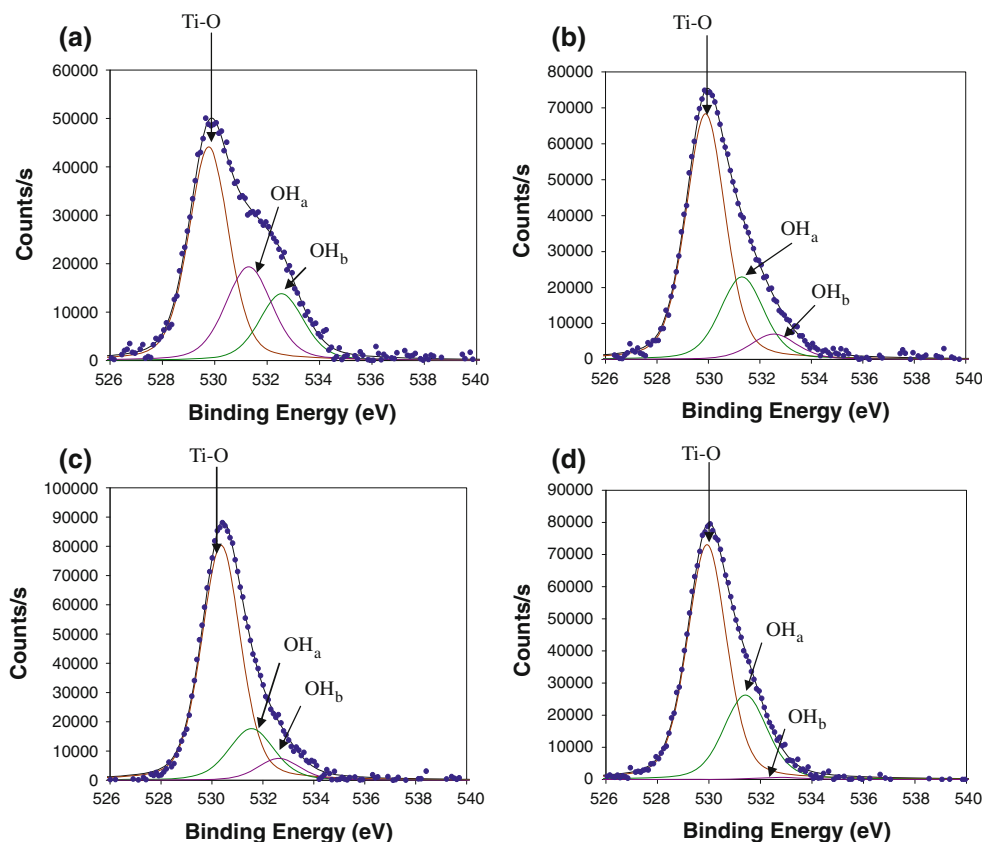


**Table 1** Peak fitting parameters in O1s region for all of the samples

	O1s (Ti–O)	O1s (acidic OH)	O1s (basic OH)
<b>Po-Ti</b>			
E <sub>b</sub> (eV)	529.8	531.3	532.6
A <sub>i</sub> (cs <sup>-1</sup> eV)	94170.47	48107.83	32732.55
A <sub>i</sub> /∑A <sub>i</sub> (%)	53.8	27.5	18.7
<b>d_Pi-Ti</b>			
E <sub>b</sub> (eV)	529.9	531.3	532.5
A <sub>i</sub> (cs <sup>-1</sup> eV)	145858	54423.2	17595.02
A <sub>i</sub> /∑A <sub>i</sub> (%)	66.9	25	8.1
<b>d_HP-Ti</b>			
E <sub>b</sub> (eV)	530.4	531.6	532.6
A <sub>i</sub> (cs <sup>-1</sup> eV)	171525	43894.27	17254.56
A <sub>i</sub> /∑A <sub>i</sub> (%)	73.8	18.8	7.4
<b>c_Pi-Ti</b>			
E <sub>b</sub> (eV)	529.9	531.4	532.8
A <sub>i</sub> (cs <sup>-1</sup> eV)	156008.4	62285.3	1650.675
A <sub>i</sub> /∑A <sub>i</sub> (%)	71	28.3	0.7

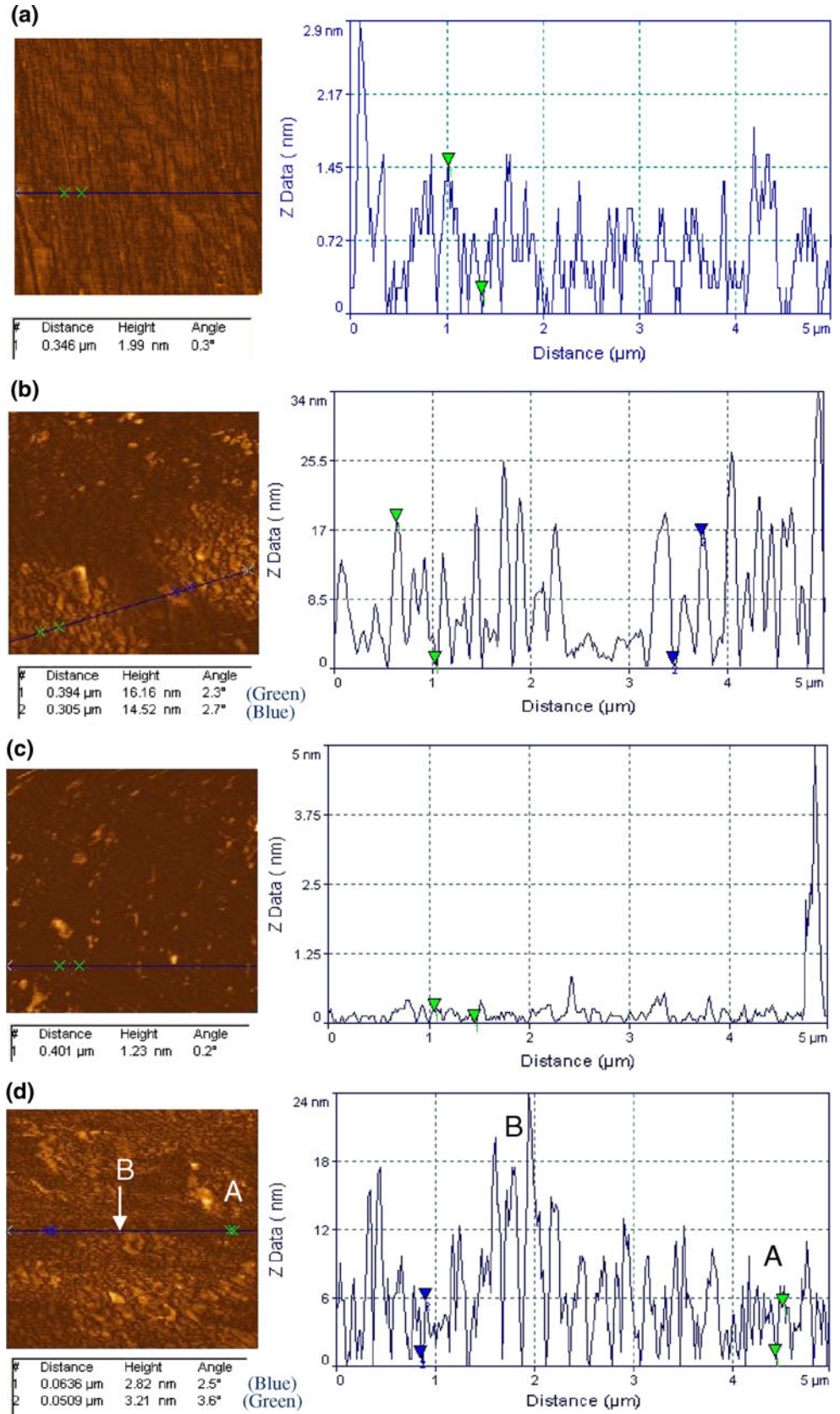
A<sub>i</sub> is the area under peak, E<sub>b</sub> is the binding energy of the peak, and A<sub>i</sub>/∑A<sub>i</sub> is the contribution of each peak in the sample

appeared to be composed of large aggregates with an average height of 15.34 nm indicating that the OTS molecules self-assembled into multilayer structures. Clearly, the initial hydrophobicity of the surface and high

hydrocarbon contaminations inhibited the formation of a monolayer at the surface of Po-Ti. In comparison, the surface of d\_Pi-Ti appeared fully covered, but the film obtained was not of uniform thickness. On some parts of the substrate, a monolayer was observed (Fig. 8, Area A, peak to valley height of 2.82 nm corresponding to the length of a fully stretched OTS), whereas a multilayer structure appeared on other parts of the substrate (Fig. 8, Area B).

The conformational disorder of the OTS film was further clarified by infrared spectroscopy (Fig. 9). According to previous investigations, highly ordered and dense monolayer of alkylsiloxane chains show stretching vibrations at 2960, 2920 and 2850 cm<sup>-1</sup> for ν<sub>as</sub>(-CH<sub>3</sub>), ν<sub>as</sub>(-CH<sub>2</sub>) and ν<sub>s</sub>(-CH<sub>2</sub>), respectively [49–52]. In the present study, only the substrates treated with the *Piranha* solution, i.e. d\_Pi-Ti and c\_Pi-Ti, displayed vibrations at 2920, 2960 and 2850 cm<sup>-1</sup>. Furthermore, the ν<sub>as</sub>(-CH<sub>3</sub>) vibration clearly observed at 2975 cm<sup>-1</sup> for d\_Pi-Ti and not with c\_Pi-Ti further confirms that most alkylsiloxane chains are vertically oriented on d\_Pi-Ti [53]. Accordingly, on d\_Pi-Ti the OTS film is more dense and ordered than on c\_Pi-Ti, where the high surface roughness may have led to enhanced steric repulsions of the alkyl chains and a certain degree of conformational disorder [53]. For d\_HP-Ti and Po-Ti, a significant shift for all stretching vibrations to

**Fig. 8** AFM images (5  $\mu\text{m} \times 5 \mu\text{m}$ ) and line analysis of (a) Po-Ti, (b) Po-Ti after OTS adsorption, and (c) d\_Pi-Ti, (d) d\_Pi-Ti after OTS adsorption





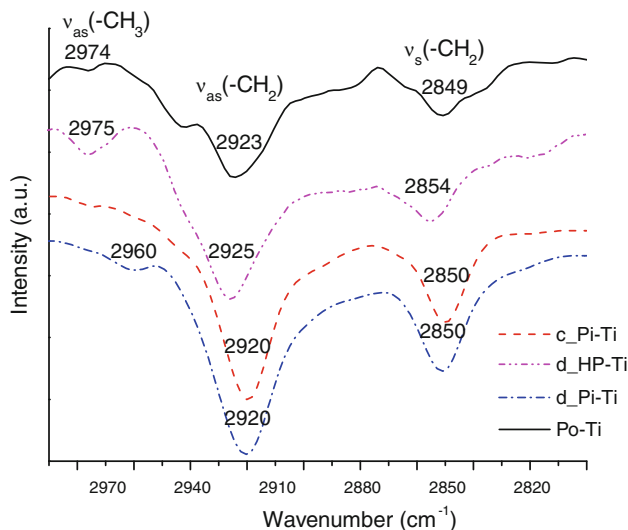


**Fig. 9** FTIR spectra of the titanium substrates after OTS adsorption in the C–H stretching region

higher frequencies was observed (Fig. 9). Therefore, the OTS molecules adsorbed on the surface of d\_HP-Ti and Po-Ti are not well-organized and most of the alkylsiloxane chains may lie on the substrate or form vertical polymeric structures [54–56].

### 4 Discussion

From these results, it can be concluded that the formation of OTS self-assembled monolayer at the surface of titanium is not as simple as previously reported. The reaction of OTS with hydroxylated surfaces is relatively complex, [54, 57] and according to previous investigations, it is not clear whether the adsorption of OTS occurs through a ligand exchange mechanism whereby the chlorosilanes are pre-hydrolyzed before the adsorption can take place (Fig. 10a), or if the adsorption reaction directly proceeds via the hydrolysis of the chlorosilanes end group by the titanium OH groups (Fig. 10b). Once in contact with titanium, the formation of an organized self-assembled monolayer of OTS molecules depends upon several parameters, including the water concentration and the density of OH on the surface of titanium [25, 54, 57]. If the reaction follows a ligand exchange mechanism, water needs to be added to the OTS solution. However, adding water would also result in the polymerization of OTS molecules and the deposition of aggregates onto the surface of titanium. In our experimental conditions, a dry hydrophobic solvent was used to avoid cross-polymerization of OTS molecules in the solution and maintain a thin layer of water molecules nearby the surface to induce the

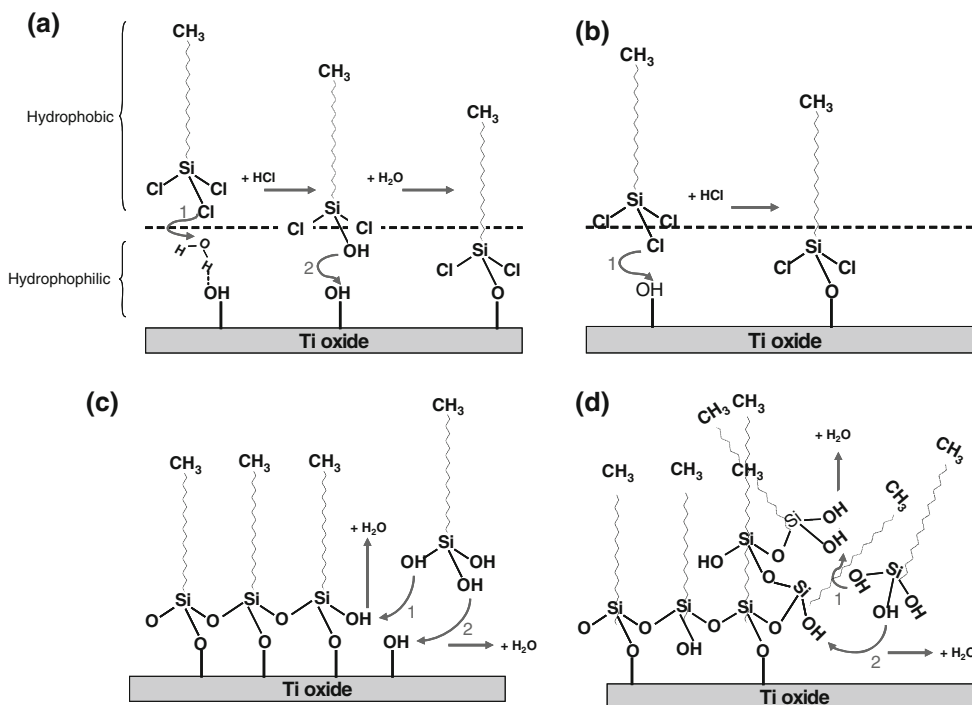


**Fig. 10** Schematic representation of the adsorption mechanism of OTS onto the surface of titanium: (a) according to a ligand exchange mechanism, (b) according to a direct hydrolysis of the chlorosilanes through the titanium hydroxyl. (c) Growth of the OTS monolayer in case of a high density of hydroxyls at titanium surface following a

ligand exchange mechanism (horizontal polymerization). (d) Growth of the OTS monolayer in case of a low density of hydroxyls at titanium surface following a ligand exchange mechanism (vertical polymerization)

adsorption of OTS. However, these ‘favorable’ conditions alone were insufficient to facilitate the formation of a consistent monolayer at the surface of titanium. In fact, our observations demonstrate that the formation of a well-organized monolayer depends more on the pre-treatment conditions than the concentration of water within the substrate-liquid interface. While the oxidation of the substrate with  $H_2O_2$  didn’t yield the formation of a well-organized OTS film, upon pre-treatments with *Piranha* solutions the formation of an ordered OTS layer was observed (Fig. 9). Since the only difference in between the two sets of experimental conditions is the final concentration of surface hydroxyls (Table 1), it can be concluded that the differences in the OTS structures observed at the surface of both substrates are probably due to dissimilar hydroxylation states. At low OH density, once a silanol has formed a bond with a surface hydroxyl, subsequent cross-polymerization with adjacent silanols will occur within the double layer at the titanium-OTS solution interface. If a surface OH site is close enough to the first adsorption site, further cross-polymerization of OTS molecules will occur in a horizontal manner and lead to a monolayer covalently bound to the titanium surface (Fig. 10c), otherwise vertical polymerization will happen with the formation of polysilane aggregates (Fig. 10d). Such behavior is highlighted by the adsorption of OTS on Po-Ti, where the presence of hydrocarbon contaminants probably inhibits the horizontal polymerization of OTS despite a large density of hydroxyl groups at the surface of titanium. Hence, once a monolayer is formed on Po-Ti, further polymerization continues on silanols at the edges of the monolayer leading to the formation of large aggregates as observed by AFM (Fig. 8b). This polymerization process is self-sustained by the water molecules constantly available in the double layer (the reaction of silanols releases water), and would explain the non-uniformity of the layers obtained.

Since relatively well-ordered structures of OTS were only obtained on substrates showing a high concentration of acidic hydroxyl groups (i.e. *Piranha* treated substrates, Table 1); the different reactivity of the titanium OH groups could also influence the adsorption behavior of OTS at the surface of titanium. As previously mentioned, OTS adsorption can either occur through ligand exchange (Fig. 10a) or hydrolysis by surface OH groups (Fig. 10b). The possible release of a proton from the surface hydroxyl would probably be the favorable adsorption path in detriment to the ligand exchange route, which involves replacing a basic surface OH with an OH from the neutrally charged silanol. Although these two reaction paths have been considered equivalent in previous investigations [54], our results suggest a molecular recognition path at the titanium-OTS solution interface, with OTS molecules recognizing specific acidic adsorption sites. Such behavior

is not unique to OTS molecules. For instance, the adsorption of complexes at the surface of silica within the solid-liquid interface has been reported to proceed through site recognition [58]. Hence, to achieve a homogeneous and full coverage of OTS molecules on the surface of titanium, pre-treatment methods promoting the formation of the acidic hydroxyl groups, rather than basic hydroxyl groups, should be derived.

## 5 Conclusions

The effect of conventional chemical pre-treatments, i.e.  $H_2O_2$  and *Piranha* solution, on the surface morphology and chemistry of titanium substrates was investigated in an attempt to rationalize the conditions for the formation of well-organized SAM films based on OTS. According to our results, a well-ordered monolayer would not be obtained even though the pre-treatment conditions are carefully controlled. For the best result, a pre-treatment with diluted *Piranha* should be used to avoid excessive corrosion of the titanium substrate and the formation of a very porous surface. Furthermore, sufficient density of hydroxyl groups at the surface of titanium appeared to be essential for the horizontal polymerization of the OTS molecules on the surface of titanium. A low hydroxyl concentration would result in vertical polymerization of the silanols groups and the formation of large aggregates. In addition, the adsorption of OTS on the surface of titanium may depend on the type of titanium hydroxyl group, i.e. acidic or basic. The formation of the covalent bonds,  $\equiv Ti-O-SiCl_2-C_xH_y$ , through the direct reaction of acidic hydroxyl groups with the chlorosilane end groups would be the favorable reaction path for the formation of a well ordered and dense SAM film at the surface of titanium.

**Acknowledgments** This work was supported by Furlong Research Foundation (and Joint Replacement Instrumentation Limited), UK.

## References

1. Sundgren JE, Bodo P, Lundstrom I. Auger electron spectroscopic studies of the interface between human tissue and implants of titanium and stainless steel. *J Colloid Interface Sci.* 1986;110:9–20.
2. Liu Q, Ding J, Mante FK, et al. The role of surface functional groups in calcium phosphate nucleation on titanium foil: a self-assembled monolayer technique. *Biomaterials.* 2002;23:3103–11.
3. Liu X, Chu PK, Ding C. Surface modification of titanium, titanium alloys, and related materials for biomedical applications. *Mater Sci Eng A.* 2004;47:49–121.
4. Furlong RJ, Osborn JF. Fixation of hip prostheses by hydroxyapatite ceramic coatings. *J Bone Joint Surg Am.* 1991;73B:741–5.
5. Yang Y, Kim KH, Ong JL. A review on calcium phosphate coatings produced using a sputtering process—an alternative to plasma spraying. *Biomaterials.* 2005;26:327–37.

6. Campbell AA, Fryxell GE, Linehan JC, et al. Surface-induced mineralization: a new method for producing calcium phosphate coatings. *J Biomed Mater Res.* 1996;32:111–8.
7. Majewski PJ, Allidi G. Synthesis of hydroxyapatite on titanium coated with organic self-assembled monolayers. *Mater Sci Eng A.* 2006;420:13–20.
8. Mao C, Li H, Cui F, et al. Oriented growth of hydroxyapatite on (0001) textured titanium with functionalized self-assembled silane monolayer as template. *J Mater Chem.* 1998;8:2795–801.
9. Masuda Y, Sugiyama T, Koumoto K. Micropatterning of anatase TiO<sub>2</sub> thin films from an aqueous solution by a site-selective immersion method. *J Mater Chem.* 2002;12:2643–7.
10. Zhu P, Masuda Y, Koumoto K. The effect of surface charge on hydroxyapatite nucleation. *Biomaterials.* 2004;24:3915–21.
11. Toworfe GK, Composto RJ, Shapiro IM, et al. Nucleation and growth of calcium phosphate on amine-, carboxyl- and hydroxyl-silane self-assembled monolayers. *Biomaterials.* 2006;27:631–42.
12. Zhu P, Masuda Y, Koumoto K. Site-selective adhesion of hydroxyapatite microparticles on charge surfaces in a supersaturated solution. *J Colloid Interface Sci.* 2001;243:31–6.
13. Zhu PX, Ishikawa M, Seo WS, et al. Nucleation and growth of hydroxyapatite on an amino organosilane overlayer. *J Biomed Mater Res.* 2002;59:294–304.
14. Tanahashi M, Matsuda T. Surface functional group dependence on apatite formation on self-assembled monolayers in a simulated body fluid. *J Biomed Mater Res.* 1997;34:305–15.
15. Zhu P, Masuda Y, Yonezawa T, et al. Investigation of apatite deposition onto charged surfaces in aqueous solutions using a quartz-crystal microbalance. *J Am Ceram Soc.* 2003;86:782–90.
16. Huang S, Zhou K, Liu Y, et al. Controlled crystallization of hydroxyapatite under hexadecylamine self-assembled monolayer. *Trans Nonferr Metal Soc.* 2003;13:595–9.
17. Zhu P, Masuda Y, Koumoto K. A novel approach to fabricate hydroxyapatite coating on titanium substrate in an aqueous solution. *J. Ceram Soc Jpn.* 2001;109:676–80.
18. Nanci A, Wuest JD, Peru L, et al. Chemical modification of titanium surfaces for covalent attachment of biological molecules. *J Biomed Mater Res.* 1998;40:324–35.
19. Schreiber F. Structure and growth of self-assembling monolayers. *Prog Surf Sci.* 2000;65:151–256.
20. Collins RJ, Sukenik CN. Sulfonate-functionalized, siloxane-anchored, self-assembled monolayers. *Langmuir.* 1995;11:2322–4.
21. Lewandowska M, Włodkowska M, Olkowski R, et al. Chemical surface modifications of titanium implants. *Macromol Symp.* 2007;253:115–21.
22. Tengvall P, Elwing H, Lundstrom I. Titanium gel made from metallic titanium and hydrogen peroxide. *J Colloid Interface Sci.* 1989;130:405–13.
23. Tengvall P, Elwing H, Sjoqvist L, et al. Interaction between hydrogen peroxide and titanium: a possible role in the biocompatibility of titanium. *Biomaterials.* 1989;10:118–20.
24. Tengvall P, Lundstrom I, Sjoqvist L, et al. Titanium-hydrogen peroxide interaction: model studies of the influence of the inflammatory response on titanium implants. *Biomaterials.* 1989;10:166–75.
25. Wang Y, Lieberman M. Growth of ultrasMOOTH octadecyltrichlorosilane self-assembled monolayers on SiO<sub>2</sub>. *Langmuir.* 2003;19:1159–67.
26. Ban S, Iwaya Y, Kono H, et al. Surface modification of titanium by etching in concentrated sulfuric acid. *Dent Mater.* 2006;22:1115–20.
27. Pan J, Liao H, Leygraf C, et al. Variation of oxide films on titanium induced by osteoblast-like cell culture and the influence of an H<sub>2</sub>O<sub>2</sub> pretreatment. *J Biomed Mater Res.* 1998;40:244–56.
28. Hammond JS, Holubka JW, DeVries JE, et al. The application of X-ray photoelectron spectroscopy: a study of interfacial composition-induced paint de-adhesion. *Corros Sci.* 1981;21:239–53.
29. Ong JL, Lucas LC, Gregory JC. Electrochemical corrosion analyses and characterization of surface-modified titanium. *Appl Surf Sci.* 1993;72:7–13.
30. Pan J, Thierry D, Leygraf C. Hydrogen peroxide toward enhanced oxide growth on titanium in PBS solution: blue coloration and clinical relevance. *J Biomed Mater Res.* 1996;30:393–402.
31. Schmidt M. X-ray photoelectron spectroscopy studies on adsorption of amino acids from aqueous solutions onto oxidised titanium surfaces. *Arch Orthop Traum Surg.* 2001;121:403–10.
32. Shirkhazadeh M. XRD and XPS characterization of superplastic TiO<sub>2</sub> coatings prepared on Ti6Al4V surgical alloy by an electrochemical method. *J Mater Sci Mater Med.* 1995;6:206–10.
33. Kilpadi DV, Raikar GN, Liu J, et al. Effect of surface treatment on unalloyed titanium implants: spectroscopic analyses. *J Biomed Mater Res.* 1998;40:646–59.
34. Pouilleau J, Devilliers D, Groult H. Surface study of a titanium-based ceramic electrode material by X-ray photoelectron spectroscopy. *J Mater Sci.* 1997;32:5645–51.
35. Takeuchi M, Abe Y, Yoshida Y, et al. Acid pretreatment of titanium implants. *Biomaterials.* 2003;24:1821–7.
36. Taborelli M, Jobin M, François P, et al. Influence of surface treatments developed for oral implants on the physical and biological properties of titanium. (I) Surface characterization. *Clin Oral Implants Res.* 1997;8:208–16.
37. Feng B, Chen JY, Qi SK, et al. Characterization of surface oxide films on Titanium and bioactivity. *J Mater Sci Mater Med.* 2002;13:457–64.
38. Lu G, Bernasek SL, Schwartz J. Oxidation of a polycrystalline titanium surface by oxygen and water. *Surf Sci.* 2000;458:80–90.
39. Brunette DM, Tengvall P, Textor M, et al. Titanium in medicine. Materials science, surface science, engineering, biological responses and medical applications. Heidelberg: Springer; 2001.
40. Feng B, Chen JY, Qi SK, et al. Carbonate apatite coating on titanium induced rapidly by precalcification. *Biomaterials.* 2002;23:173–9.
41. Sham TK, Lazarus MS. X-ray photoelectron spectroscopy (XPS) studies of clean and hydrated TiO<sub>2</sub> (Rutile) surfaces. *Chem Phys Lett.* 1979;68:426–32.
42. Boehm HP. Acidic and basic properties of hydroxylated metal oxide surfaces. *Faraday Discuss.* 1971;52:264–75.
43. Matsumura K, Hyon S, Nakajima N, et al. Adhesion between poly(ethylene-co-vinyl alcohol) (EVA) and titanium. *J Biomed Mater Res.* 2002;60:309–15.
44. Blesa MA, Weisz AD, Morando PJ, et al. The interaction of metal oxide surfaces with complexing agents dissolved in water. *Coord Chem Rev.* 2000;196:31–6.
45. Tamura H, Mita K, Tanaka A, et al. Mechanism of hydroxylation of metal oxide surfaces. *J Colloid Interface Sci.* 2001;243:202–7.
46. Wang LQ, Baer DR, Engelhard MH, et al. The adsorption of liquid and vapor water on TiO<sub>2</sub> (110) surfaces: the role of defects. *Surf Sci.* 1995;344:237–50.
47. Kulkarni SA, Mirji SA, Mandale AB, et al. Growth kinetics and thermodynamic stability of octadecyltrichlorosilane self-assembled monolayer on Si(100) substrate. *Mater Lett.* 2005;59:3890–5.
48. Ulman A. Formation and structure of self-assembled monolayers. *Chem Rev.* 1996;96:1533–54.
49. Abdelghani A, Hleli S, Cherif K. Optical and electrochemical characterization of self-assembled octadecyltrichlorosilane monolayer on modified silicon electrode. *Mater Lett.* 2002;56:1064–8.
50. Collet J, Vuillaume D. Nano-field effect transistor with an organic self-assembled monolayer as gate insulator. *Appl Phys Lett.* 1998;73:2681–3.

51. Hoffmann H, Mayer U, Krischanitz A. Structure of alkylsiloxane monolayers on silicon surfaces investigated by external reflection infrared spectroscopy. *Langmuir*. 1995;11:1304–12.
52. Mirji SA. Adsorption of octadecyltrichlorosilane on Si(100)/SiO<sub>2</sub> and SBA-15. *Colloids Surf A*. 2006;289:133–40.
53. Yasseri AA, Sharma S, Kamins TI. Alkylsiloxane self-assembled monolayer formation guided by nanoimprinted Si and SiO<sub>2</sub> templates. *Appl Phys Lett*. 2006;89:10–153121.
54. Fadeev AY, McCarthy TJ. Self-assembly is not the only reaction possible between alkyltrichlorosilanes and surfaces: monomolecular and oligomeric covalently attached layers of dichloro- and trichloroalkylsilanes on silicon. *Langmuir*. 2000;16:7268–74.
55. Khatri OP, Biswas SK. Boundary lubrication capabilities of alkylsilane monolayer self-assembled on aluminium as investigated using FTIR spectroscopy and nanotribometry. *Surf Sci*. 2006;600:4399–404.
56. Parikh AN, Allara DL. An intrinsic relationship between molecular structure in self-assembled *n*-alkylsiloxane monolayers and deposition temperature. *J Phys Chem B*. 1994;98:7577–90.
57. Rye RR, Nelson GC, Dugger MT. Mechanistic aspects of alkylchlorosilane coupling reactions. *Langmuir*. 1997;13:2965–72.
58. Boujday S, Lambert JF, Che M. Bridging the gap between solution and solid-state chemistry molecular recognition at the liquid–solid interface. *Top Catal*. 2003;24:37–42.